Petroleum Science
https://doi.org/10.1007/s12182-020-00442-0

ORIGINAL PAPER

Deep-water depositional architecture and sedimentary evolution in the Rakhine Basin, northeast Bay of Bengal

Hong-Xia Ma[1] · Guo-Zhang Fan[1] · Da-Li Shao[1] · Liang-Bo Ding[1] · Hui Sun[1] · Ying Zhang[1] · Yong-Gang Zhang[1] · Bryan T. Cronin[2]

Received: 21 March 2019

Abstract
Since the consecutive discovery of several gas fields from 2004 to present, the Rakhine Basin has been an active area for petroleum exploration in the Bay of Bengal. High-resolution 3D seismic data and well data from blocks AD1, AD6 and AD8 offshore northwest Myanmar are used to study the Miocene–Pleistocene depositional architecture and sedimentary evolution in the Rakhine Basin. Analysis of seismic facies and seismic attributes indicates that deep-water architectural elements include submarine canyons, confined slope channel complex systems, aggradational channel–levee complexes, isolated channels, frontal splays and mass-transport complexes, which have variable characters (shape, dimension, sedimentary architecture) within predominantly background deep-water slope-basin floor facies. Most of the sediments are interpreted to be sourced from the Ganges–Brahmaputra fluvio-deltaic system to the north with only minor lateral input from the Indo-Myanmar Ranges to the east. Investigation of the depositional evolution and architectural elements transformation during the filling history of the Rakhine Basin suggests the Rakhine Basin experienced rapid progradation during the Oligocene–Middle/Upper Miocene, gradual retrogradation during the Middle/Upper Miocene–Early Pliocene and gradual progradation during the Early Pliocene–Pleistocene. Published exploration results indicate that the main reservoirs of the discoveries in blocks A1 and A3 are Pliocene frontal splays and channel–levee fills, dominated by fine and very fine-grained sandstones, in structural and structural–stratigraphic traps. Analytic results from seismic characters and several exploration wells indicate that channel complexes and associated overbanks and frontal splays with fine-grained sandstones and siltstones trapped by the four-way closures are primary reservoir targets.

Keywords Bengal fan · Rakhine basin · Architectural element · Sedimentary evolution

1 Introduction

The Bengal Fan, the largest submarine fan on Earth covering the floor of all of Bay of Bengal (Hübscher et al. 1997; Weber et al. 1997), has attracted extensive attention from petroleum geologists in recent years. Several large discoveries have been made (Mya, Shwe, Shwe phyu and Thalin) in northeast part of the Bengal Fan, offshore Rakhine Basin, Myanmar, in the past decades. In 2004, biogenic gas-charged Pliocene turbidites were penetrated in several wells, and the Shwe, Shwe Phyu and Mya gas fields were discovered in blocks A1 and A3 (Yang and Kim 2014). Since then, the Rakhine Basin, which comprises shelf-slope blocks A1–A7 & AD6 and slope to deep-water blocks AD1–AD5 & AD7–AD16 (Fig. 1a) (Racey and Ridd 2015), has been the focus of deep-water exploration. However, little has been published on the detailed deep-water depositional architecture and evolution of the Rakhine Basin, although some publications have been presented to improve the understanding of architecture and growth processes of the northeast Bengal Fan during the past 20 years (Curray et al. 2002; Hübscher et al. 1997; Schwenk et al. 2005; Subrahmanyam et al. 2008; Weber et al. 2003). Here, we offer a key paper that includes new data with observations and interpretations based on industry seismic and well data to describe the seismic facies

Edited by Jie Hao

✉ Hong-Xia Ma
mahx_hz@petrochina.com.cn; hongxiama@foxmail.com

[1] PetroChina Hangzhou Research Institute of Geology, Hangzhou 310023, Zhejiang, China

[2] Deep Marine Ltd, 9 North Square, Footdee, Aberdeen AB11 5DX, Scotland, UK

Published online: 20 April 2020

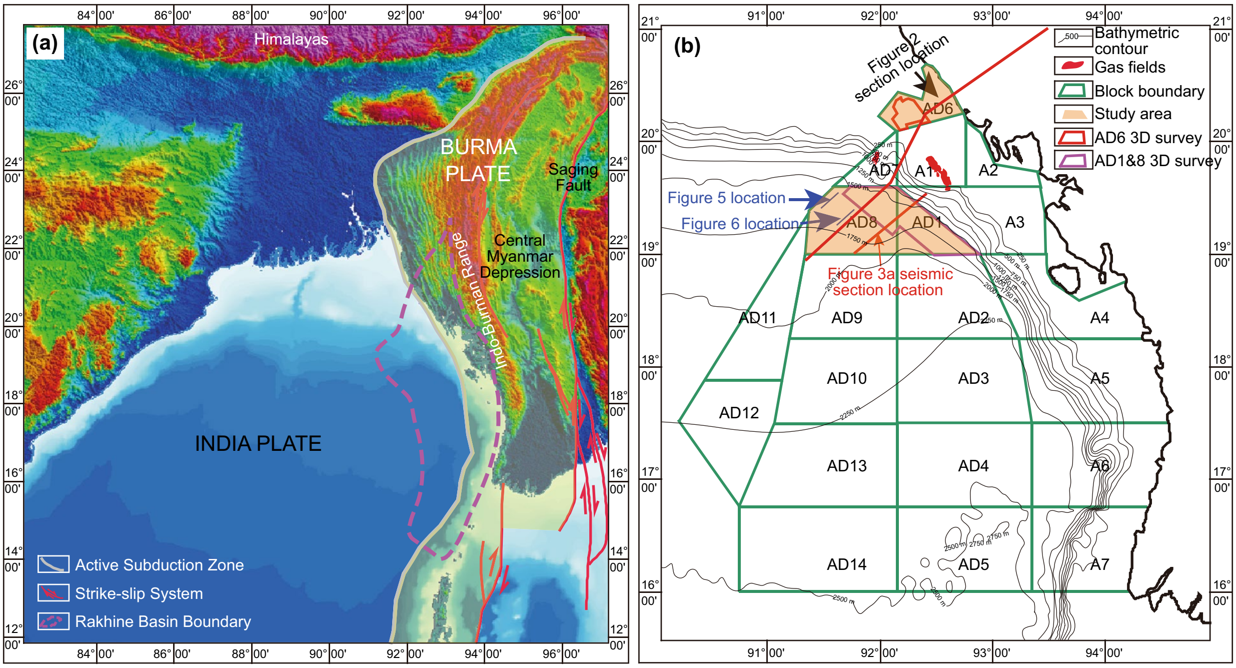

Fig. 1 Location map of the Rakhine Basin (**a**), showing main tectonic provinces in the northeastern Bay of Bengal, and location map of the study area (**b**), illustrating exploration blocks, discovered gas fields and bathymetry (Racey and Ridd 2015)

and architectural elements of the Miocene–Pleistocene found in shelf Block AD6 and slope deep-water blocks AD1&8 (Fig. 1b).

The objectives of this paper are to (1) use high-resolution 3D seismic imaging to characterize the geometry and internal architectures of a portion of the palaeo-Bengal Fan; (2) preliminarily summarize a depositional model of a fine-grained deep-water system; (3) illustrate the deep-water depositional evolution and discuss the controlling factors and the provenance variation; and (4) discuss the implications for hydrocarbon exploration of the Rakhine Basin.

2 Basin overview

The Rakhine Basin is a Tertiary foredeep basin located along the eastern fringe of the Bay of Bengal and the western coastal provinces of Myanmar (Fig. 1a). It is predominantly an offshore basin, with the onshore parts comprising low-lying islands and coastal areas.

The formation of the Rakhine Basin is closely related to oblique convergence of the Indian and Burmese Plates from the Paleocene, with the ensuing westward migration of the developing accretionary wedge (Indo-Burma Range). Current basin includes the young folded and thrusted sequences of the accretionary wedge (Pliocene-present), which formed as a result of oblique subduction of the oceanic Indian Plate beneath the island arc/forearc silver of the Burmese Plate and undeformed submarine sequences. Simplistically, three structural belts are evident in the basin based on the tectonic deformation intensity, including fold and thrust belt, gentle fold belt, and undeformed abyssal plain belt from east to west (Fig. 2). The western margin of deformed sequences is defined by the accretionary wedge front, which is deformed by a combination of transform and compressional movements.

The basin is thought to contain over 12,000 m of sediment fill of Upper Cretaceous-Holocene. Tertiary exposure in the present onshore portion of the basin contain open marine and near shore to deltaic sediments, while the offshore portion contains continental shelf, slope and basin floor facies.

3 Database and methods

The study areas AD6, AD1 and AD8, located across the shelf and basin floor of the central part of Rakhine Basin, are at water depths of less than 100 m on the shelf (Block AD6), and 1300–2100 m on the slope to basin floor (Block AD1&8).

The data set used for this research is a conventional, industry, 3-D seismic volume with a dominant frequency of 40 Hz in shelfal areas to 30 Hz in the slope-basin floor areas. Line spacing is 12.5 m in cross-line directions and 25 m in inline directions. The studied interval is from Pleistocene to

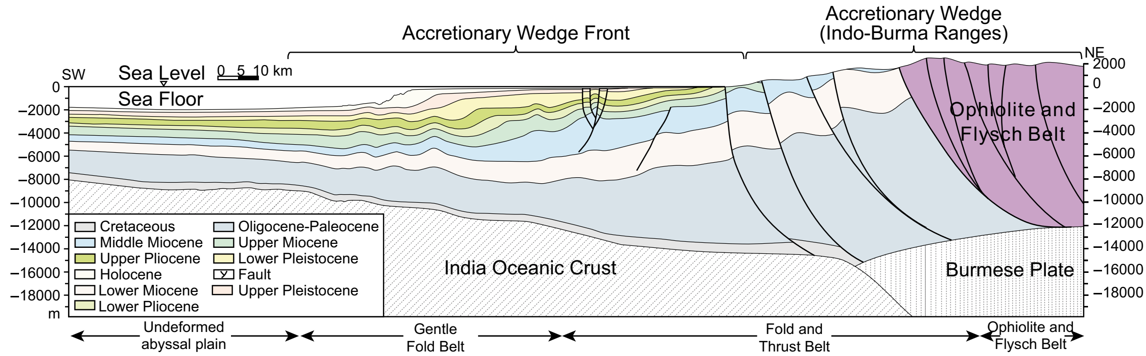

Fig. 2 Regional sketch section across the northern Rakhine Basin (refer to Fig. 1b for the location of this section)

Miocene. This interval ranges in thickness from 4000 m in Block AD1&8 to as much as 5500 m in Block AD6.

All of the seismic images in this paper are displayed in SEG positive standard polarity, in which a positive reflection coefficient is represented by a central peak (plotted black) and troughs are red. Fortunately, there are boreholes in the study areas and adjacent areas to calibrate seismic interpretation with lithology. Lithologies drilled by wells range from fine-grained sandstones, siltstones to mudstones. Well data indicate that the acoustic impedance of sandstones from seabed to Miocene is distinctly lower than that of mudstones and there are no carbonate and volcanic sediments in the study areas. In general, the high amplitudes observed on the seismic data are associated with fine-grained sandstones and siltstones, the tops of which correspond to the amplitude troughs.

The reflection events in the studied interval have low-moderate continuity with high amplitude within a background of low-amplitude–transparent seismic facies (Fig. 3a). A schematic stratigraphic sections for the Tertiary of the deep-water Rakhine Basin show the architectural elements and general depositional evolution in light of the general seismic characters observed in Block AD1&8 (Fig. 3b).

The high-resolution 3D seismic data are used to recognize the profile features of the architectural elements, and the best images from horizontal slices generated from 3-D seismic amplitude cube and 3-D semblance cube provide a useful method for defining the elements' forms and geometries (Li et al. 2017b). And the lithology can be predicted by the seismic inversion combined with the well calibration.

4 Deep-water architectural elements

The deep-water system of Miocene–Pleistocene in the Rakhine Basin is observed to comprise six distinct and contrasting deep-water architectural elements: (1) submarine canyon, (2) confined slope channel complex system, (3) aggradational channel levee complex, (4) frontal splay (depositional lobe), (5) isolated channel, and (6) mass-transport complex (MTC) (Table 1). These elements are recognized from their geometries, seismic facies and well data. The following section focuses on these architectural elements and their seismic facies.

4.1 Submarine canyon

Submarine Canyons are large-scale erosional features up to 850 m deep and 10 km wide (Fig. 4a) with variable internal seismic geometries and are mainly observed in the northern Block AD6. A key aspect of submarine canyons in this area in particular is that they are found located in shelfal areas in the Pliocene–Pleistocene, with delta front deposition characterized by high amplitude and parallel reflections in seismic below the canyons' erosional bases (Fig. 4b, c) and multiple-thickening upwards sequences observed on gamma ray well profiles of fine-grained sandstones–siltstones. The bases of the canyons are often highly irregular with stepped, erosional, staircase trajectories. In plan form, the canyons form a tributary network with steep-sided, smaller erosional gullies feeding into a larger trunk canyon. The canyon fill seismic character contrasts starkly with the seismic facies they truncate. Three principal seismic facies within the shelf canyon fills are recognized (Fig. 4b, c): SF1—low-amplitude to transparent or chaotic reflection packages predominate; SF2—discontinuous, high-amplitude seismic reflections characterized by either vertically or laterally offset-stacked V- or U-shaped channel elements that are arranged in variably stacked clusters; SF3—medium- to low-amplitude reflections of limited lateral extent, found at similar stratigraphic levels to SF2 seismic facies or the upper part of the canyon fillings.

The canyon is observed almost everywhere to erode into high-amplitude topset, or shelfal (shallow marine) substrate. These underlying seismic facies are high- to moderate-amplitude, tramline seismic facies with continuous

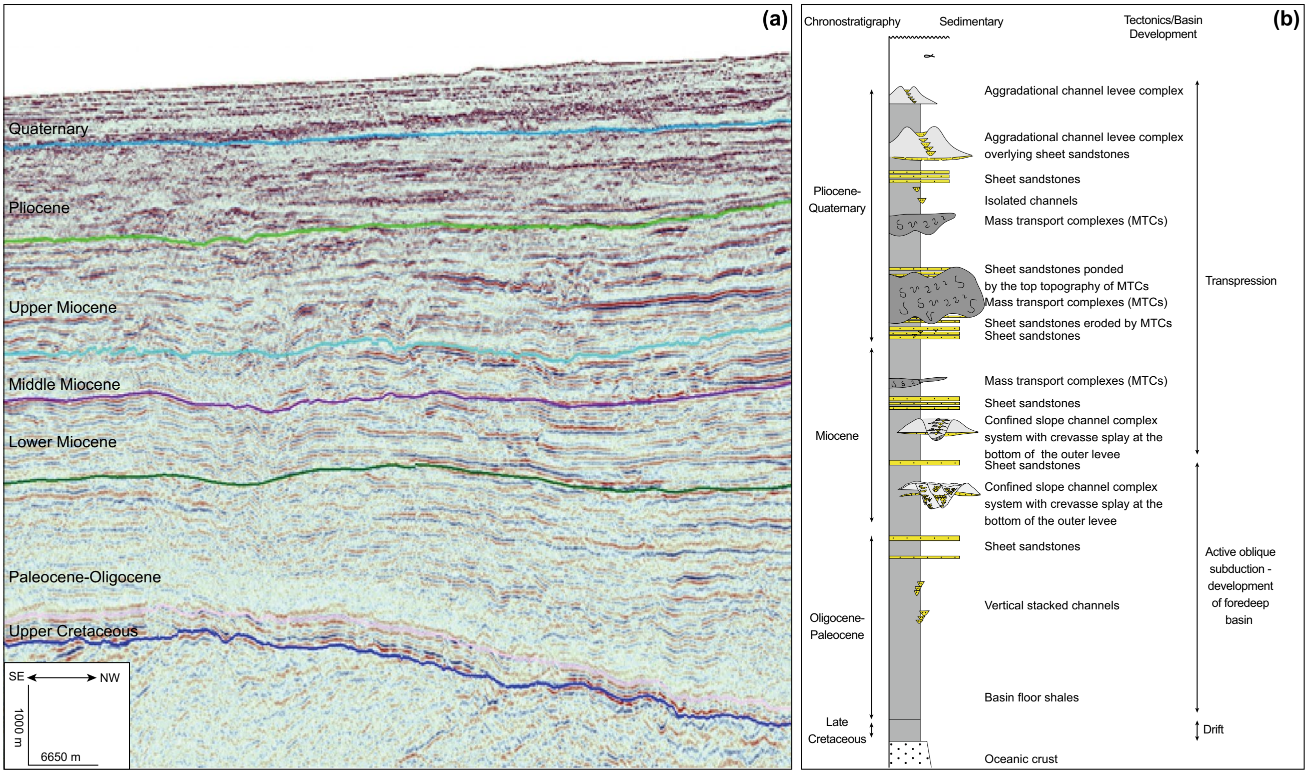

Fig. 3 **a** SE–NW seismic section across the western offshore deep-water part of Rakhine Basin illustrating deep-water strata thickness and seismic facies (refer to Fig. 1b for the location of the seismic section). **b** Stratigraphy column for the offshore deep-water part of Rakhine Basin. Schematic stratigraphic column showing deep-water lithology and typical architectural elements observed from the seismic

parallel seismic reflections. A series of proximal–distal transects through one of the main Pleistocene submarine canyons, which shows a number of features, are displayed. Firstly, the head area is characterized by a series of tributary gullies which pass down dip into a single submarine canyon (Fig. 4a). The average erosional depth is approximately 400–500 m. Secondly, the canyons are associated with syn-sedimentary faulting at the canyon margins, as so often with submarine canyons (Twichell et al. 1995), with a series of depositional terraces seen outboard of the canyon axis-directed faults.

SF1 seismic facies is interpreted as fine-grained sediments dominated by slumps generated by failure of the canyon margins, or longer distance transportation of muddy/silty debris flows from further up the canyon. SF2 seismic facies is interpreted as stacked sand-filled turbidite channel elements. SF3 seismic facies are interpreted as passive filling of the canyon by fine-grained turbidites and hemipelagic shales, either as canyon-wide drapes or inside levee wedges associated with late-stage meandering channel elements. Thus, the canyons are predominantly fine-grained as observed in well penetrations, with a combination of slumps, and fine-grained inside levee or lateral canyon quiescent drape facies commonly enveloping the various stacked or isolated channel elements.

The canyons in Block AD6 propagated progressively shelfwards, perhaps even shorewards from Miocene to Pleistocene by retrogressive headwards failure due to avalanching (Xu et al. 2014). This is evidenced by the gross erosional character of the canyons, with large-scale syn-sedimentary margin failure excavating the growing features through a series of avalanches. Significant proximal portions of the larger canyons are found in a shallow marine context (Belderson and Stride 1969; Belderson and Kenyon 1976). In addition, canyons progressively shift and young from east to west. This is thought to be due to the westward shift of fluvial input to the north, and tectonic uplift to the east resulted from westwards-migration of the accretionary wedge.

4.2 Confined slope channel complex system

Confined slope channel complex systems (CSCCS) are observed downslope from submarine canyons in the study area. They comprise a wide erosional fairway element, flanked by aggradational levee wings. The erosional fairway element is the main defining element seen seismically,

Table 1 Typical features of six architectural elements in the study area

Architectural Element	Profile	3D view or plan view	Seismic Facies	Logging	Description
Submarine Canyon	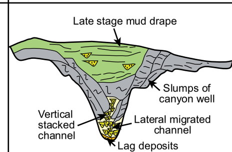	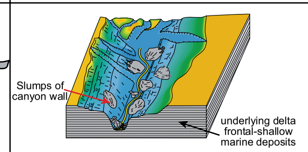	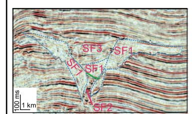	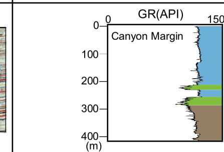	Large scale erosional features with variable internal seismic geometries. Internal seismic facies can be classified into three types: SF1-low amplitude -transparent chaotic reflectors; SF2-discontinuous, high amplitude seismic reflectors; and SF3-medium-low amplitude reflectors of limited lateral extent. The gamma ray log pattern in the canyon margin is shaly interbedded with sands. The internal fill can be divided into four stages: stage 1-erosion and sediments bypass; stage 2-mixed erosion and deposition, featured by lateral migrated channels; stage 3-paticularly commom slumps blocked the canyon, generating the dominantly vertical stack of channels; stage 4-mudstone passive filling
Confined Slope Channel Complex System	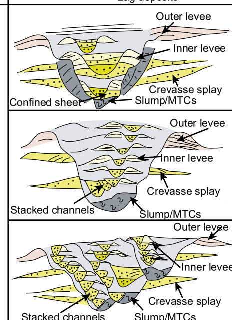	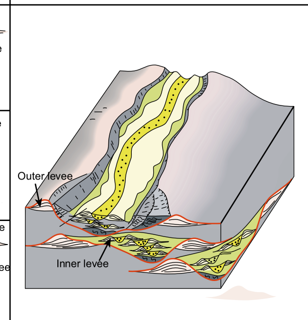	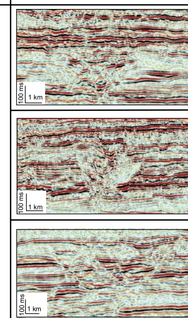	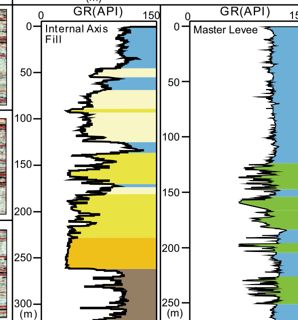	The erosional fairway element is a large and prominent incision flanked by wedge-shaped outer levees. Channel-axis deposits are characterized by discontinuous high amplitude reflectors that are formed by lateral and vertical migration of coarse-grained channel thalweg deposits. Inner levees are characterized by chaotic, or transparet low amplitude reflectors with a stepped shape. Seismic reflections within outer levees are always continuous, but can range from low to high amplitude. The wireline-log pattern in the internal axis fills composed of high GR at the base suggesting mud prone, blocky sands at the lower part and thin/fine upward to shale pattern at top. On the gamma-ray log, the master levees consist of interbedded sands and shales at the lower part and fine upwards to shales at the upper part.
Aggradational Channel Levee Complex	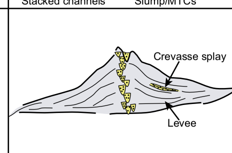	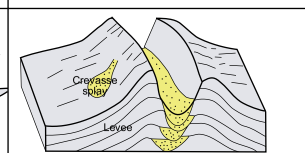	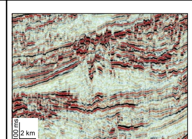	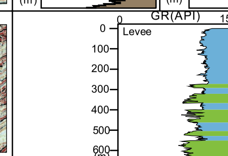	Levee sediements are characterized by low amplitude, continuous and/or relatively transparent reflectors with a double-wedge shape that thins away from the channel-fill sediments that characterized by high amplitude discontinuous reflectors on seismic. The gamma-ray log response of levee is generally shaly or “ratty” in appearance, more sandy pattern at the lower pattern and shows vertical decrease in grain size and N:G.
Isolated Channel	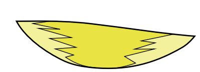	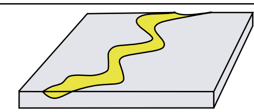	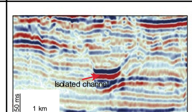	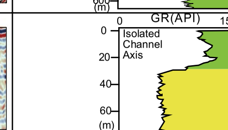	The seismic facies is characterized by high amplitude, discontinuous reflectors. The planeform can be highly sinuous Typical wireline-log pattern is blocky at the lower part and fines upward to shales at the top.
Frontal Splay	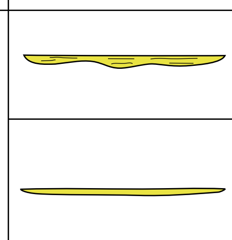	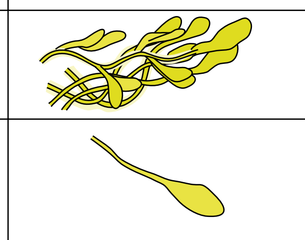	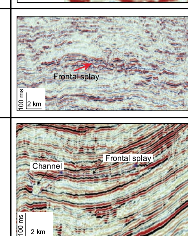	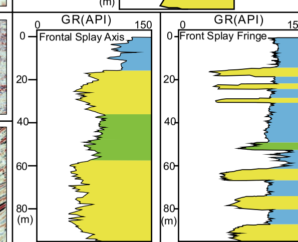	Frontal splays appear as one to several parallel to sub-parallel, high amplitude reflectors with moderate to good continuity. Frontal splays have a variety of shapes in the study area, such as elongate or radial geometry. The gamma ray log pattern consists of blocky with sharp base at the front splay axis and a more serrated pattern for more distal frontal splays.
Mass Transport Complex	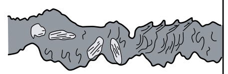	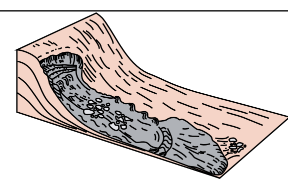	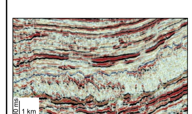	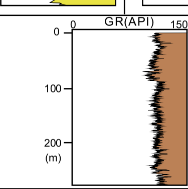	The seismic facies is characterized by chaotic to hummocky reflectors with poor continuity and variable amplitude with obvious erosional base surface and irregular top surface. The gamma ray log pattern is generally shaly.

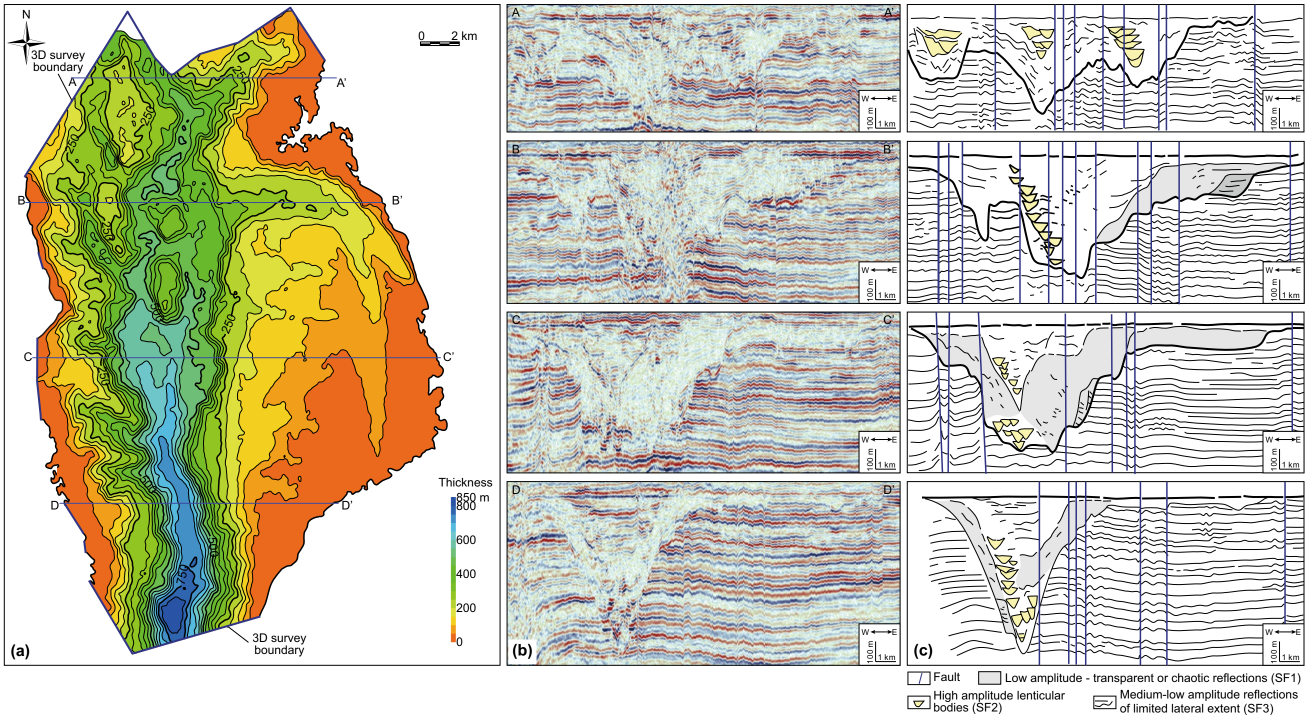

Fig. 4 Isopach map (**a**) of a Pleistocene submarine canyon from Block AD6, showing a series of tributary gullies in the head area, four strike lines (**b**) and the geological interpretation (**c**) showing the seismic facies changes down dip the flow direction

observed as a large and prominent incision scour flanked by wedge-shaped outer, or master, levees. The width of the erosional fairway element exceeds 5.5 km, and the thickness exceeds 540 m (Fig. 5). The thicker axial parts of the CSCCS are characterized by discontinuous, high-amplitude reflections arranged as laterally lenses that can be mapped as moderately sinuous channels on planform seismic slices. Seismic reflections within outer flanking wedge-shaped master levees are almost always continuous, but can range from low to high amplitude.

Some of the CSCCSs are isolated (Fig. 5), and some are observed to be multiple, stacked erosional–depositional systems (Fig. 6). In Block AD1&8, these multiple CSCCSs comprise discontinuous, mainly high-amplitude reflection bundles contained within three or more obvious, and mappable, U-shaped erosion surfaces and the seismic bundles clearly display different stacking patterns. The total width of these CSCCSs exceeds 8 km, whereas the typical width and thickness of the mappable channel complex set inside them are 2 km and 300 m, respectively (Fig. 6).

The erosional fairway element within the CSCCS is interpreted as the main pathway for turbidity currents, which initially bypass the channels and deposit coarse-grained lags. The fill of the erosional fairway is dominated by lateral and vertical migration of channel thalweg deposits that have high-amplitude seismic character and are interpreted as coarse-grained lags. Inner levees associated with them are characterized by chaotic or transparent low amplitude reflections with a stepped shape. The edges of the erosional fairway are characterized by stepped terraces, often capped by fine-grained facies. These bench-like depositional terraces can form from both depositional processes (i.e., vertical aggradation of inner levee deposits resulting from the overbanking of under-fit channels) and erosional processes (i.e., sculpting and slumping of inner levees along channel margins) (Gong et al. 2016, 2018). The attached wedges outboard of the erosional fairways of the slope channel complexes are interpreted as master, or external levees that correspond to aggradational phases of the channel complexes where fine-grained sediments overspilled the margins.

CSCCSs prevail in Miocene sediments in Block AD1&8. They have either vertically offset-stacked, laterally stacked or a combination of entrenched and offset-stacked channel complexes within them, forming channel complex systems (Figs. 5, 6). Confined slope channel complex systems are well-known features in the subsurface (often called slope channel complexes, valleys-fills, confined slope channel complexes, or confined slope channel complex systems) (Cronin et al. 2005; Janoko et al. 2013; Kang et al.2018; Sprague et al. 2005). In this paper, we refer to them as Confined Slope Channel Complex Systems. The terminology ascribed to these features, particularly the hierarchy of recognizable architectural element. CSCCSs are the downslope continuation of submarine canyons. CSCCSs differ from

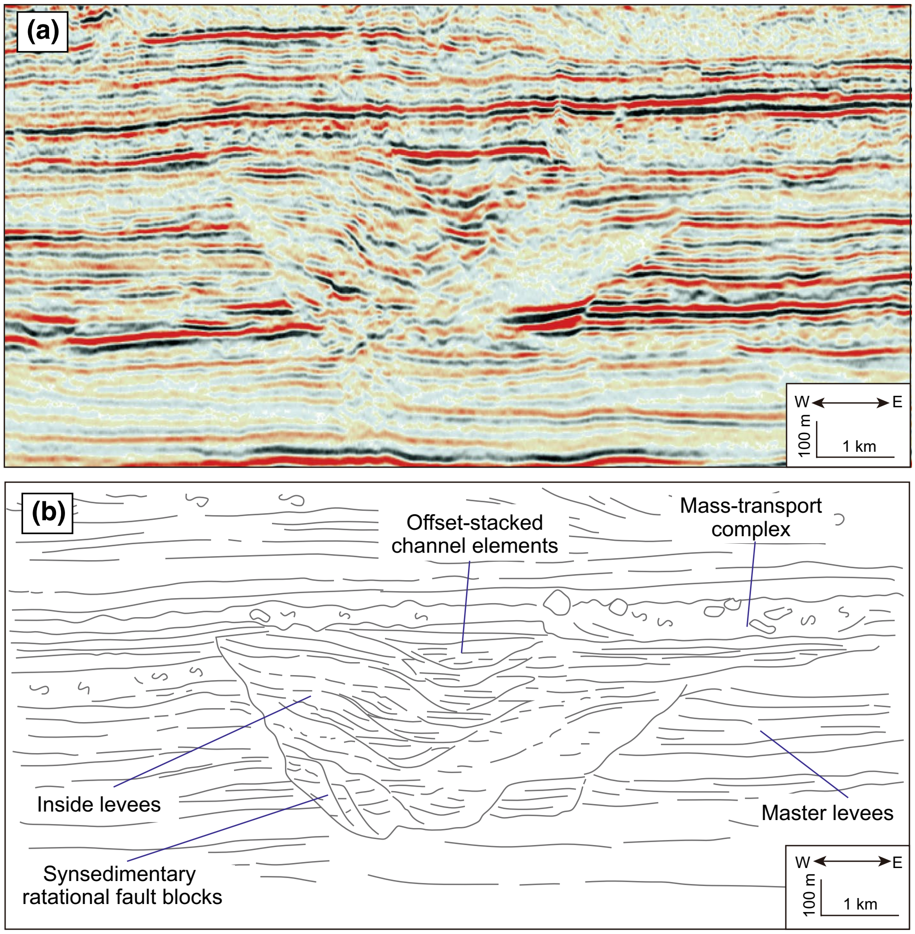

Fig. 5 Seismic facies (**a**) and geological interpretation (**b**) showing an entrenched variant of confined slope channel complex system. Seismic facies comprise chaotic, discontinuous, mixed low and high-amplitude reflectors. Sub-environments include the main erosional fairway (with a single master erosional surface), channel-axis deposits (with offset-stacked channel elements), inside levees and master levees (refer to Fig. 1b for the location of this section)

submarine canyons by their general confinement—where canyons are strictly entirely or mostly erosional, CSCCSs have an earlier erosional or entrenched phase followed by a combined confined/aggradational master levee growth phase, and smaller scale contained channels and inner levees filling phase. Furthermore, the range of stacking patterns within a CSCCS from the proximal area to the distal area is observed in the study to be variable. As shown in Fig. 7, in the proximal area of the CSCCS from the Upper Miocene is a classic 'entrenched channel complex' (Cronin et al. 2005); further downslope, the CSCCS breaks out into three laterally offset CSCCS; and even further downdip, there are more resolvable CSCCSs. The lateral migration of the entire CSCCS is thought to be related to a gradual increase in accommodation space downslope, allowing reoccupancy phases of the CSCCS to shift laterally due to lower aggradation of the enveloping master levees. The CSCCSs have a less linear planform shape further downslope and internally have more pronounced sinuous channel elements within them (Liu et al. 2013), as the degree of internal erosion, confinement, and perhaps slope and thalweg gradient, also decreases.

4.3 Aggradational channel levee complex

Aggradational channel levee complexes are mainly observed in Pliocene–Pleistocene in Block AD1&8. On seismic profiles, channel axis sediments are often characterized by high-amplitude, discontinuous reflections. Levee-overbank sediments are characterized by low-amplitude, continuous, and/or relatively transparent reflections with a double-wedge shape that thins away from the channel-fill sediments. The thickness-to-width (aspect) ratio of these levee units varies significantly from system to system. The maximum width of these facies reaches up to 23 km, whereas the general thickness is approximately 340 m (Fig. 8). The stacking patterns in these aggradational channel complexes are variable but

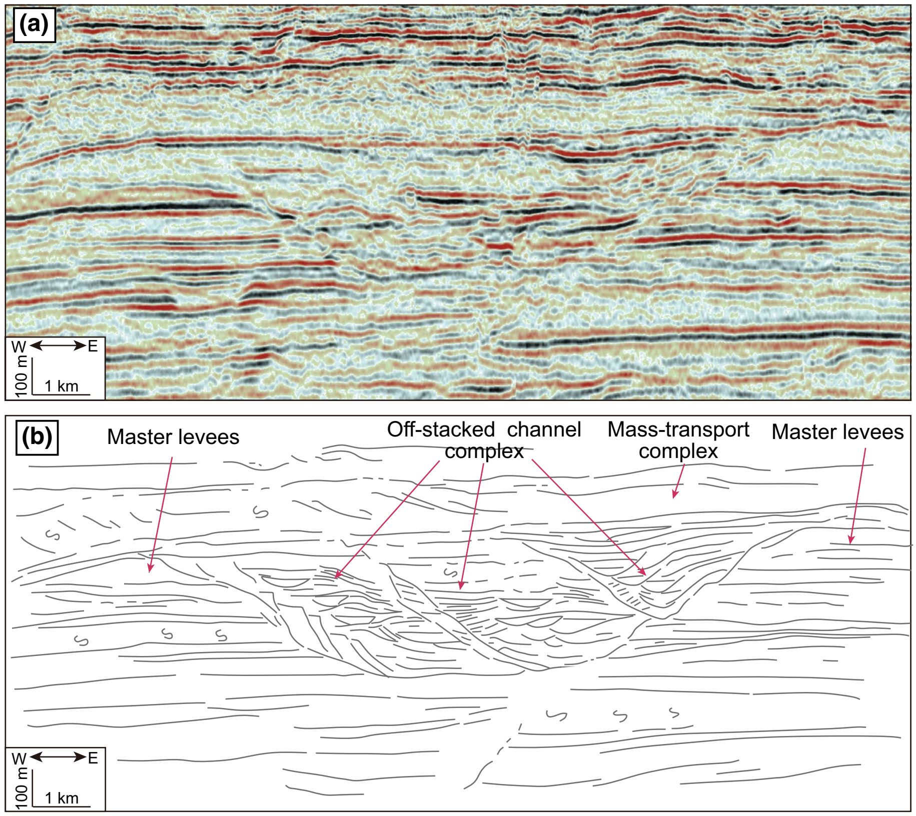

Fig. 6 Seismic facies (**a**) and geological interpretation (**b**) of a laterally stacked confined slope channel complex system. Here, each successive phase has a master erosional surface, internal vertically and laterally offset-stacked channel elements, and internal and master levees (refer to Fig. 1b for the location of this section)

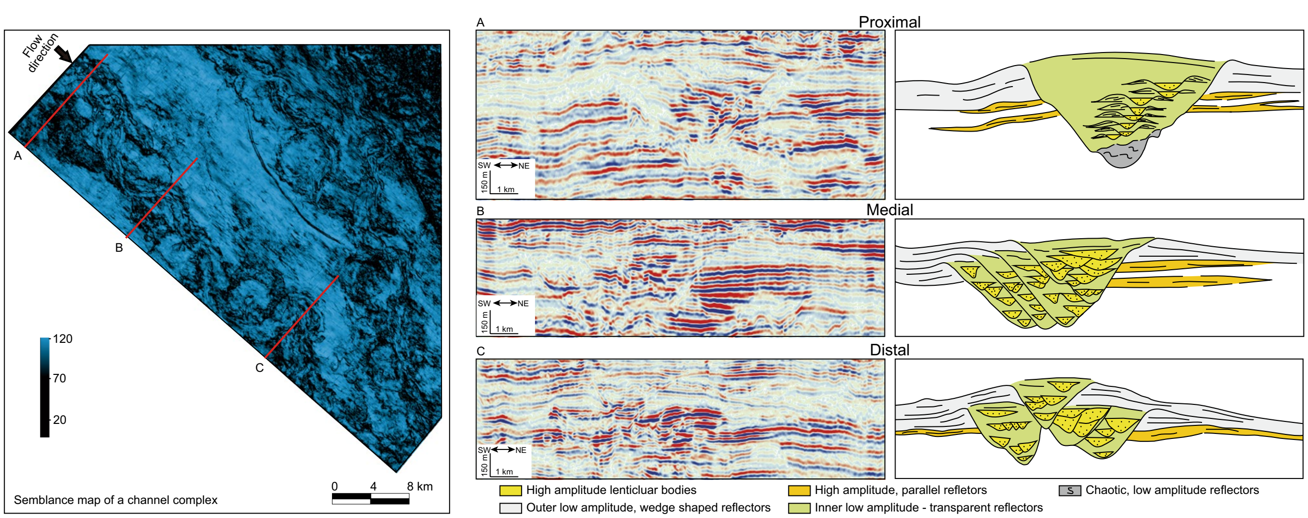

Fig. 7 Semblance map (**a**) and downslope transformation (**b**) of a confined slope channel complex system

dominated by channel elements that initially stack laterally and then progressively stack vertically.

The levee can be subdivided into proximal levee, distal levee, and crevasse splay that may be comprise different sediments and have different reservoir potential. The units primarily consist of mudstones; however, thinly bedded fine-grained sandstones and siltstones also can also be deposited on these areas, which are proved by wells and characterized

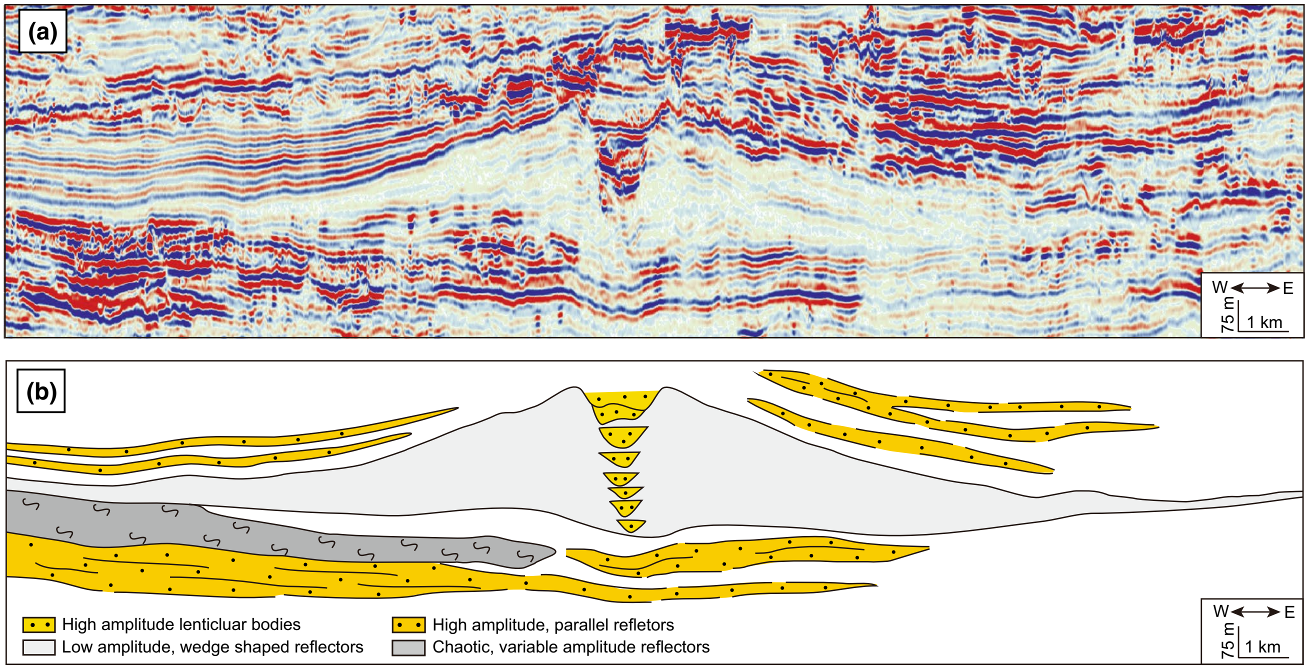

Fig. 8 Seismic facies (**a**) and interpretation (**b**) of an aggradational channel levee complex

by relatively high-amplitude reflection in seismic. The net gross can reach as much as 57% in proximal levees and 6% in distal levees from the interpretation of borehole coring in adjacent blocks. The stacking pattern of the channel elements is interpreted to reflect progressive confinement by levees.

Aggradational channel levee complexes have been described from most modern large-scale ‘passive margin’ settings since their discovery on the Amazon, Indus and Mississippi Fans (Pickering et al. 1986; Damuth et al. 1988; Pirmez et al. 1997; Kolla 2007; Kolla and Coumes 1987), and on the Bengal Fan (Curray et al. 2002; Schwenk et al. 2005; Kolla 2007). Levee-overbank sediments are mainly developed in aggradational channel–levee systems which are associated with high channel sinuosity, lower slope gradient, large terrestrial drainage basin area, and fine-grained sediment contributing to the high volume of suspended material in turbidity currents that build up these types of deep-water channel system.

4.4 Frontal splay

In Block AD1&8, frontal splays can be found at or near the base of slope, where they are usually larger and more radial, and further out on the basin floor where they are narrower and smaller. On seismic, frontal splays appear as one to several parallel, high-amplitude reflections with moderate to good continuity, often with rapid lateral terminations. However, in planform view, they have a variety of shapes such as lobate (or tongue/tab-shaped), elongate (Fig. 9) or radial (Fig. 10). The total width of these elements exceeds 8 km and the thickness exceeds 100 m in some areas. The updip contact between frontal splays and channels is transitional or unclear. We found it more convenient to put the end members of frontal splay geometries as either elongate frontal splays (for thinner, more extended frontal splays fed by narrow channels) or clustered frontal splays (for radial or lobate geometries) (Zhang et al. 2017a). More elongate frontal splays appear to be more intimately associated with channels which are narrow and bordered by a ‘double-track’ of higher amplitudes, and they are often more sinuous channels than the clustered frontal splays. Clustered frontal splays are often stacked and characterized by discontinuous high-amplitude reflections with a composite thickness of 200 m (Fig. 10a). Such a thick pile of sediments must have been deposited as a vertical stack of multiple frontal splays, as the individual splay ranges from 5 to 15 m in thickness (Lee et al. 2002; Jegou et al. 2008; Saller et al. 2008). A detail dissection displayed three stages of frontal splays as shown in Fig. 11. Each stage is separated by the low-amplitude reflection on seismic. From the bottom to the top, the proportion of channel increases. These channels are moderately sinuous with depths of 30–50 m and widths of 200–800 m.

The seismically imaged splays are resolved to geobodies which are composite in nature, being made up of smaller-scale lobe elements. These lobe elements are part of what we call the ‘invisible architecture.’ These form the flow units or genetic units within frontal splay.

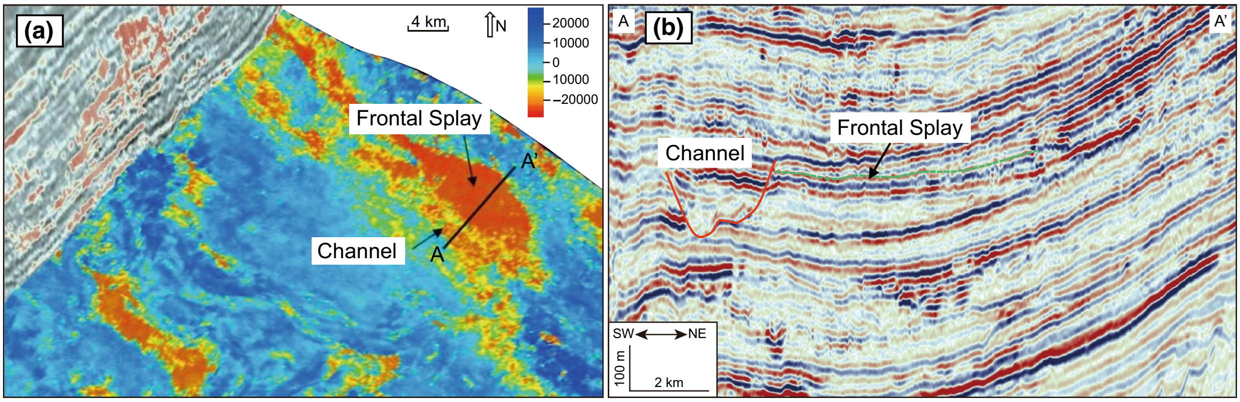

Fig. 9 Root-mean-square amplitude image (**a**) and seismic facies (**b**) of an elongate frontal splay

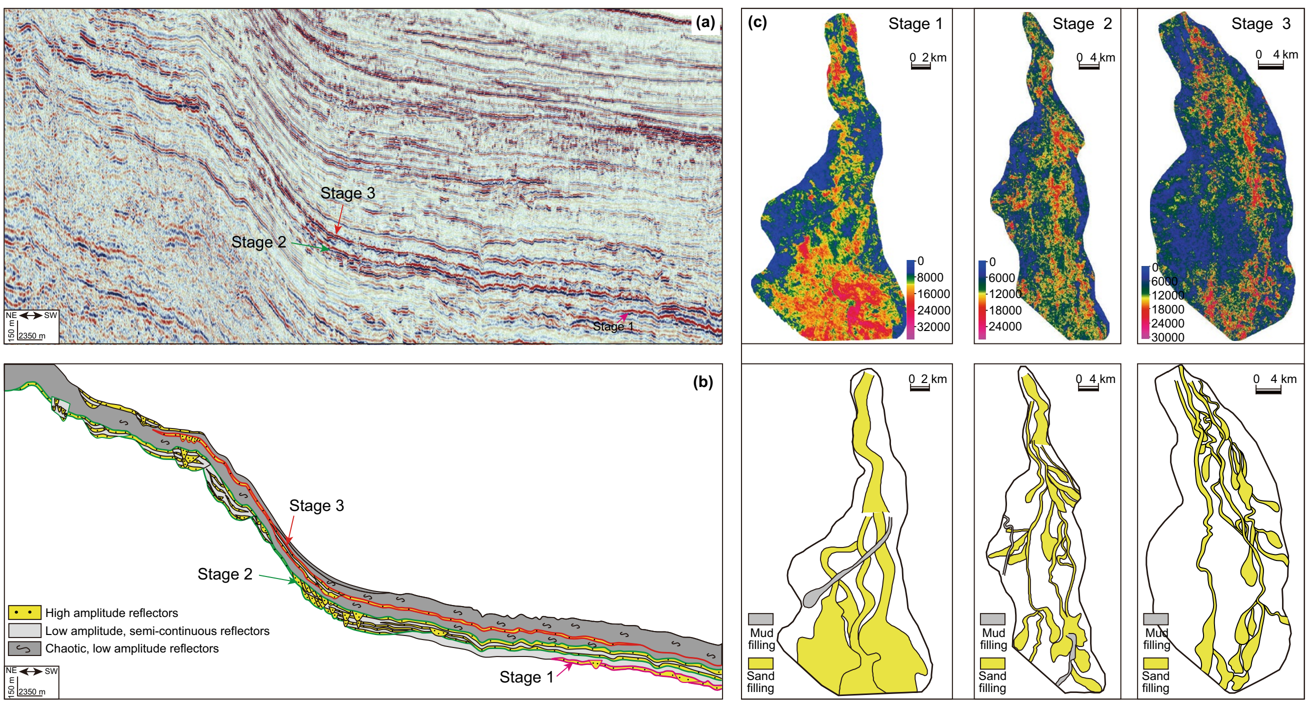

Fig. 10 Seismic facies (**a**), geological interpretation (**b**) and RMS attribute maps and interpretations (**c**) of three-stage frontal splays with associated channels and vertical variation. One of the key aspects of these sedimentary bodies is that individual flow units comprise separate splay elements which are not resolvable on seismic—what is imaged are composite splay bodies, with varying degrees of internal connectivity (RMS = root mean square)

The clustered and elongate frontal splay end members described above must always be considered as being made up of these smaller-scale elements, each 5–15 m thick on average, 1–2 km wide and 2–7 km long depending on the type of frontal splay. Though often blocky gamma ray log character, very thin shale breaks are often found between the splay elements, which form pressure seals in compartmentalization in some cases within these frontal splay reservoir bodies, or unexplained slow or tortuous communication between bodies which appear, or are assumed to be, more sheet-like in nature.

Frontal splay is a term that we adopt here for what are usually called depositional lobes. This is primarily because the term depositional lobe does not imply any strict notion of scale (Shanmugham and Moiola 1991), being a very generic term for shape; a term too embroiled in delta terminology with which there is little analogy; and which does not have an associated, widely accepted hierarchical scheme for its architectural elements. In this paper, we use the term

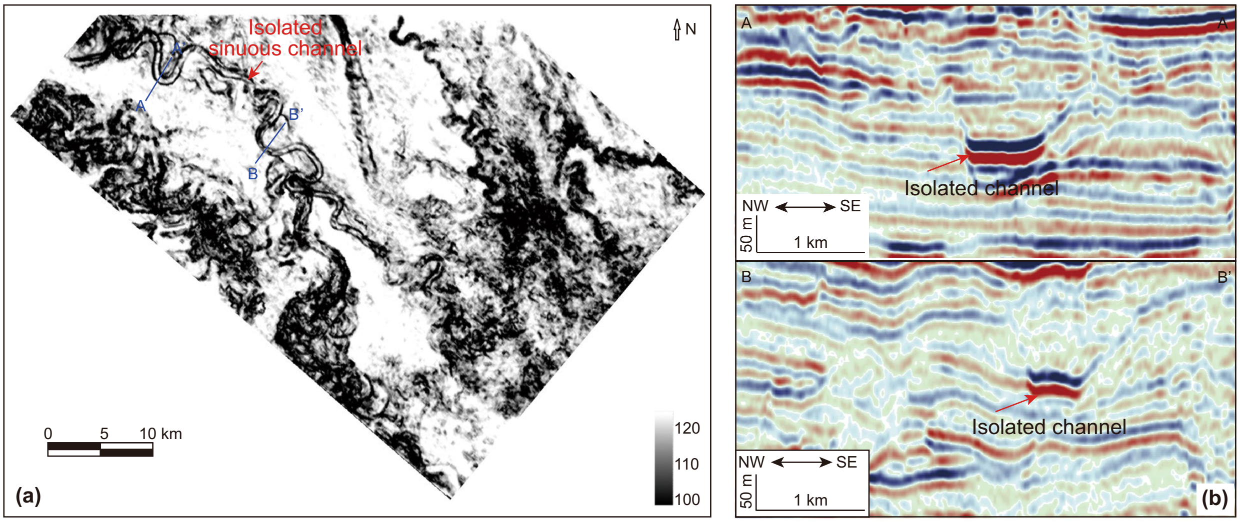

Fig. 11 Semblance attribute map (**a**) and seismic facies (**b**) of an isolated channel

frontal splay to define the depositional architectural elements that are deposited from decelerating flows at the terminus of channels (Twichell et al. 1992; Saller et al. 2008; Yang and Kim 2014) and reflect the sediments that have bypassed through updip channels (typified by confined flows) and are deposited in primarily an unconfined setting.

4.5 Isolated channel

In Block AD1&8, isolated channels are characterized by high-amplitude, discontinuous reflections (Fig. 11). Some isolated channels have pronounced levees, but many do not. According to their outer morphology, isolated channels can be highly sinuous in the study area.

Isolated channels occur in the study area, which do not fit into the CSCCS or aggradational channel levee complex definitions. An isolated channel is formed by repeated gravity flow deposits along one channel over a period of time (Zhang et al. 2017c). Isolated channels are smaller than confined channel complex systems and are not seen directly associated with frontal splays and are thus described as a separate distinct architectural element.

4.6 Mass-transport complex (MTC)

Large MTCs are mainly observed in the north and the east of Block AD1&8. The seismic facies of mass-transport complexes is primarily characterized by chaotic to hummocky reflections with poor continuity and variable amplitude. Most of these chaotic packages are characterized by dim or transparent seismic reflections, locally with inclined or cross-cutting seismic patterns, in mappable lenses with rapid lateral terminations, though some have bright amplitudes that are moderately continuous (Fig. 12).

Although unconfirmed by drilling, this range of reflectivity and continuity may result from (1) rafted blocks and clasts in debris-flow deposits; (2) variable sand content in this dominantly silty/muddy section; or (3) differential compaction that resulted in higher impedance contrasts with the enveloping, usually fine-grained sediments. In some areas, this facies bundles have erosive based where the MTCs are slightly incised into underlying sediments. In the study area, their maximum width and thickness exceed 22 km and 400 m, respectively (Fig. 12b).

Mass-transport complexes (MTCs) are sediments that have been re-sedimented by subaqueous mass-wasting processes (slumps, slides and large-scale debris-flow processes, often all in close association). Mass-transport complexes are formed by the gravity flow either down the continental slope, through submarine canyons or CSCCSs, from tectonically uplifted slope areas or laterally from canyon or confined slope channel margins. They are most commonly triggered by a range of geological processes, including tectonism, sedimentary loading, tsunami, dissociation of solid gas hydrates, storms, tidal or other longshore currents, or sea level changes (Wu et al. 2011; Qin et al. 2013). In the Bay of Bengal, mass-transport complexes have not been reported in great detail from the Bengal Submarine Fan (Ma et al., 2011), though they are important exploration targets in the Rakhine Basin (e.g., Thalin Field in Block AD7). Judging from the broad areal extent, great thicknesses of mass-transport complexes and the depositional area in the study areas, they could develop from collapse of the shelf edge and upper slope from the north, which may be result from the rapid

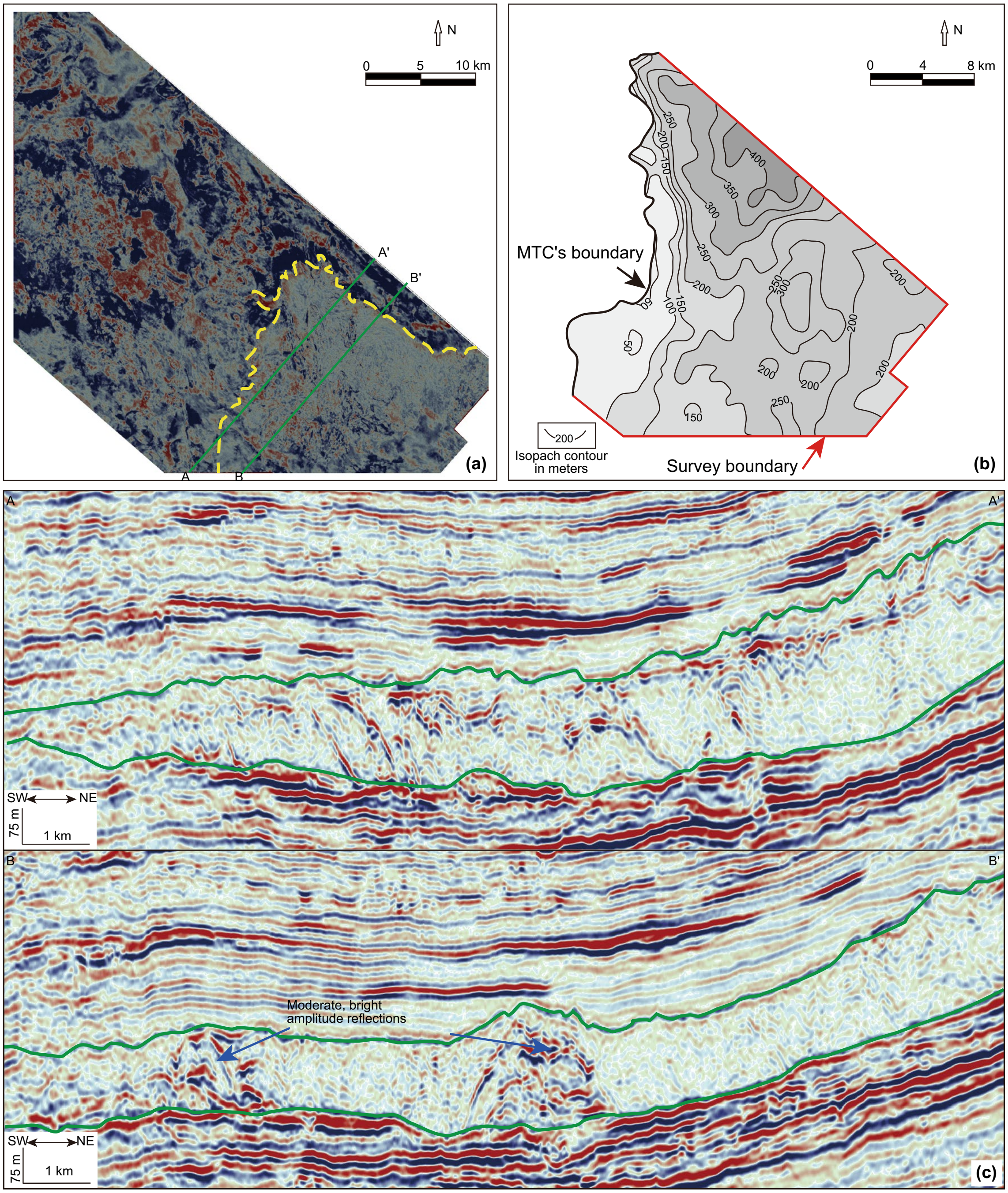

Fig. 12 Amplitude attribute map (**a**), isopach map (**b**) and seismic facies (**c**) of the mass-transport complex (MTC) in the study area

progradation of shelf deltas and the high accumulation of slope, and slumps from the east, which may be related to the relative strong tectonic activities to the east area.

4.7 Depositional model

A depositional model of the northeast Bay of Bengal is shown in Fig. 13, showing the main architectural elements in planform. This is the typical planform expression of a fine-grained deep-water system. A single deposystem is active at any one time. Six different types of deep-water architectural elements, which range in character from slope facies to basin floor facies, reflect a combination of active (sediment input from canyon/channel systems) and relatively passive (slope failures and slumps) sediment supply systems in the study area.

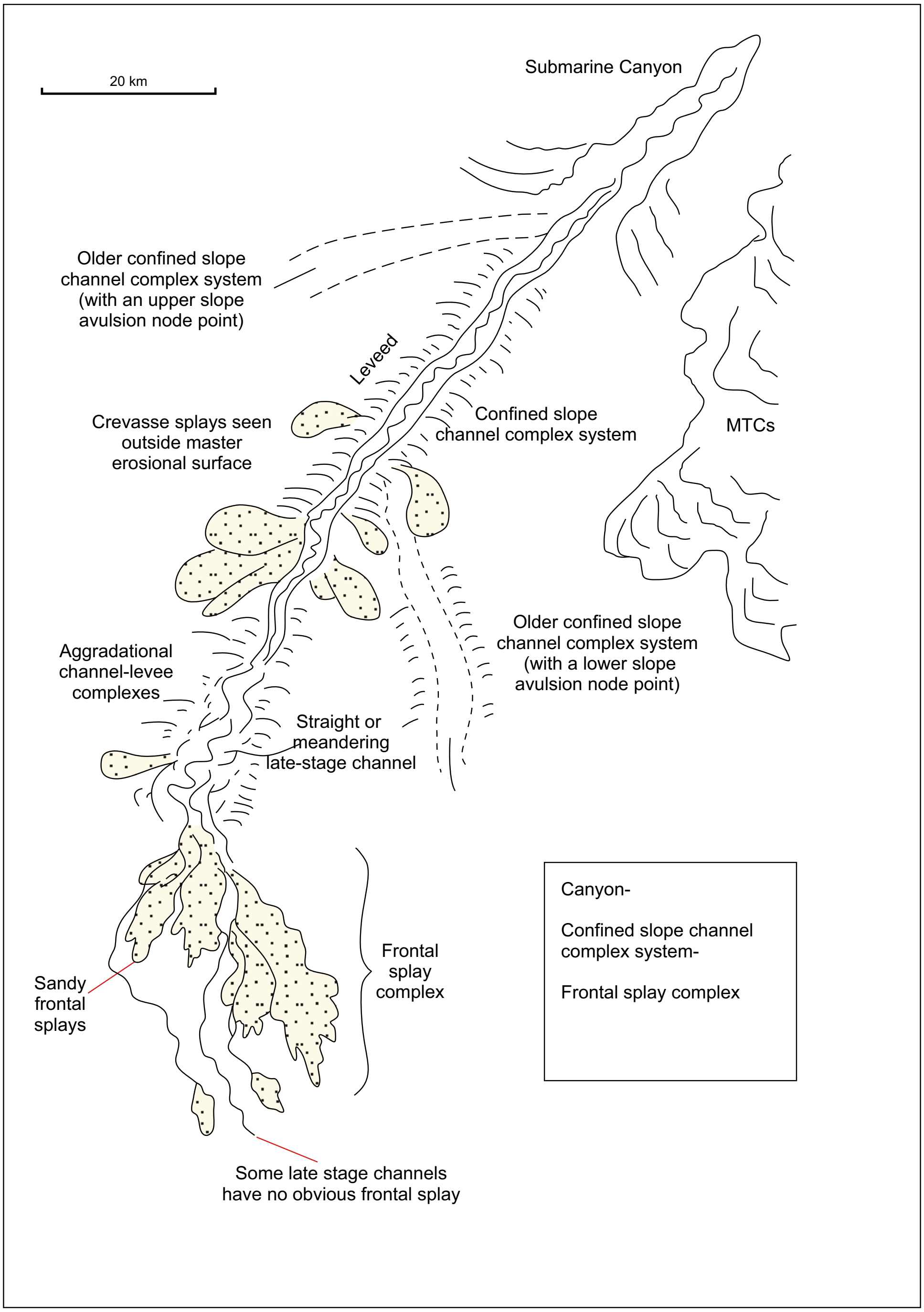

Fig. 13 Plan form model for deep-water architectural element distribution of the Rakhine basin, offshore Myanmar. Submarine canyons, confined slope channel complex systems, aggradational channel levee complexes and MTCs feature prominently. Isolated channels have not been penetrated by any wells as yet and their downdip relationship with splays is not known

5 Evolutionary history of the depositional systems

Examining the distribution of the various depositional architectural elements and the evolution of the basin fill from Eocene to Pleistocene, has been undertaken in some detail in this work. Broadly, the Eocene–Oligocene was dominated by the accumulation of hemipelagic mudstones, with no known examples of large-scale sand prone architectural elements such as confined slope channel complex systems or frontal splays recognized. The Early–Late Miocene swathe development of all of these features within an envelope of hemipelagic mudstones. Some of the frontal splays were incised into by later channels. The Lower Pliocene was dominated by the development of confined slope channel complex systems, aggradational channel levee complexes, and locally by frontal splays and hemipelagic deposits. The Upper Pliocene–Pleistocene comprised widespread aggradational channel levee complexes, frontal splays, mass-transport complexes, and hemipelagic deposits. But in Block AD6, an early Pliocene delta front began to develop from the north, and prograded southwards through late Pliocene to Pleistocene, which were incised by large-scale submarine canyons.

Investigation of depositional evolution suggests that during the Oligocene–Middle/Late Miocene the Rakhine Basin experienced rapid progradation of the deep-water slope (Zhang et al. 2017b; Li et al. 2017a), and deep-water architectural elements varied from Eocene–Oligocene hemipelagic mudstone drape to Middle/Upper Miocene confined slope channel complex systems. During the Middle/Late Miocene–Early Pliocene, the Rakhine Basin experienced gradual retrogradation and more frontal splays developed in the Lower Pliocene than those in Upper Miocene. During the Early Pliocene–Pleistocene, the Rakhine Basin experienced gradual progradation and architectural elements varied from Pliocene aggradational channel levee complexes and frontal splays to the Pleistocene aggradational channel levee complexes, submarine canyons and a delta system.

A regional strike section of the northeast part of the Bengal Fan is shown in Fig. 14, with the principal deep-water architectural elements interpreted. The switch from the confined channel complex systems in Miocene to Pliocene–Pleistocene aggradational channel levee complexes is in response to both internal factor changes in flow size, density and grain-size (Kneller 2003) and external factor changes in slope gradient, sea level and climate. Confined slope channel complex systems are characteristics of much of the Miocene, indicating the input of large volumes of gravity flow-driven resedimentation events during that time. The increase in sediment input could be due to uplifting in Himalayas and resultant steep gradient of the shelf to deep water. The increase in volume of aggradational channel levee complexes and MTCs from the Pliocene–Pleistocene, indicates an increase in volume of clay and silt. These less erosional flows could be due to the decrease in tectonic activity and the resultant decrease in steepness of the shelf to deep water. Moreover, the flows containing more silt and clay are likely to have been fed directly by hyperpycnal flows from delta distributary channels during flood and monsoon events. These flood-driven, sustained low-density turbidity currents would have an associated high volume of suspended sediment load, dominating the system. Glacio-eustatic sea level changes must also have superimposed on this progressive background change in regional tectonics (uplift of the Himalayas since Eocene and uplift of the Indo-Burmese Range to the east), climate change (related to the larger-scale plate tectonics) and vegetation in the hinterland.

Block AD-6 is characterized by multiphasic stacked canyon fills, which are typical character of upper slope-shelf facies. The N–S-trending canyon fills were sourced from the north-northwest. Besides the canyons, the discovery of shelf-edge deltas capping the canyon fills which prograde toward the west confirms the existence of provenance from the east inland Myanmar (Fig. 15). Depositional evolution from the Eocene to Pleistocene shows the southward shift of the shelf, and N–S-trending channels indicate the sediments mainly come from the north. However, we have also seen some lateral input from Myanmar, particularly in the form of low-stand deltas from the east in Block AD6 (Fig. 15). In Block A1/A3 (adjacent blocks and the sites of discovery of the Pliocene gas fields Shwe, Shwe Phyu and Mya), seismic stratigraphic analysis suggested two provenances in the Late Pliocene, one from the northwest as part of the Bengal Fan (Yang and Kim 2014) and one from the east inland Myanmar.

6 Implications for hydrocarbon exploration in the Rakhine Basin

The commercial fields were discovered to date to be biogenic gas fields produced from Pliocene structural and structural-stratigraphic traps (Shwe, Shew Phyu and Mya in Block A1&A3). In distal shelf-basin floor, the Pliocene and Miocene stratigraphic-structural traps and structural traps are predominant because of relatively weak tectonic deformation. The Pliocene and Miocene submarine fan sandstones comprise the most promising reservoirs, and hemipelagic shales provide intra-formational seals. In the Shwe field, the Pliocene basin floor fine-grained sandstones of the frontal splay comprise the main reservoir. A number of such sand bodies with good lateral continuity have been identified, and logs and core samples have indicated excellent reservoir quality for the sands, with average net-to-gross ratio of 86%, porosity of 28% and permeability of 278 md (Yang and Kim 2014). The drilling results in these adjacent blocks indicate that the main reservoirs of the discoveries are Pliocene depositional frontal splays (called depositional lobes by Yang and Kim 2014) and channel–levee–overbank sediments. The analytic results indicate that Miocene–Pliocene channel complex systems and associated overbanks and frontal splays that include fine-grained sandstones and siltstones trapped by the four-way closures are good reservoir targets. Besides, MTCs are common in the Miocene–Pleistocene, crevasse splays and frontal splays within supra- and pre-MTC unconformity forming the stratigraphic traps are indicated to provide secondary reservoir targets. Other plays

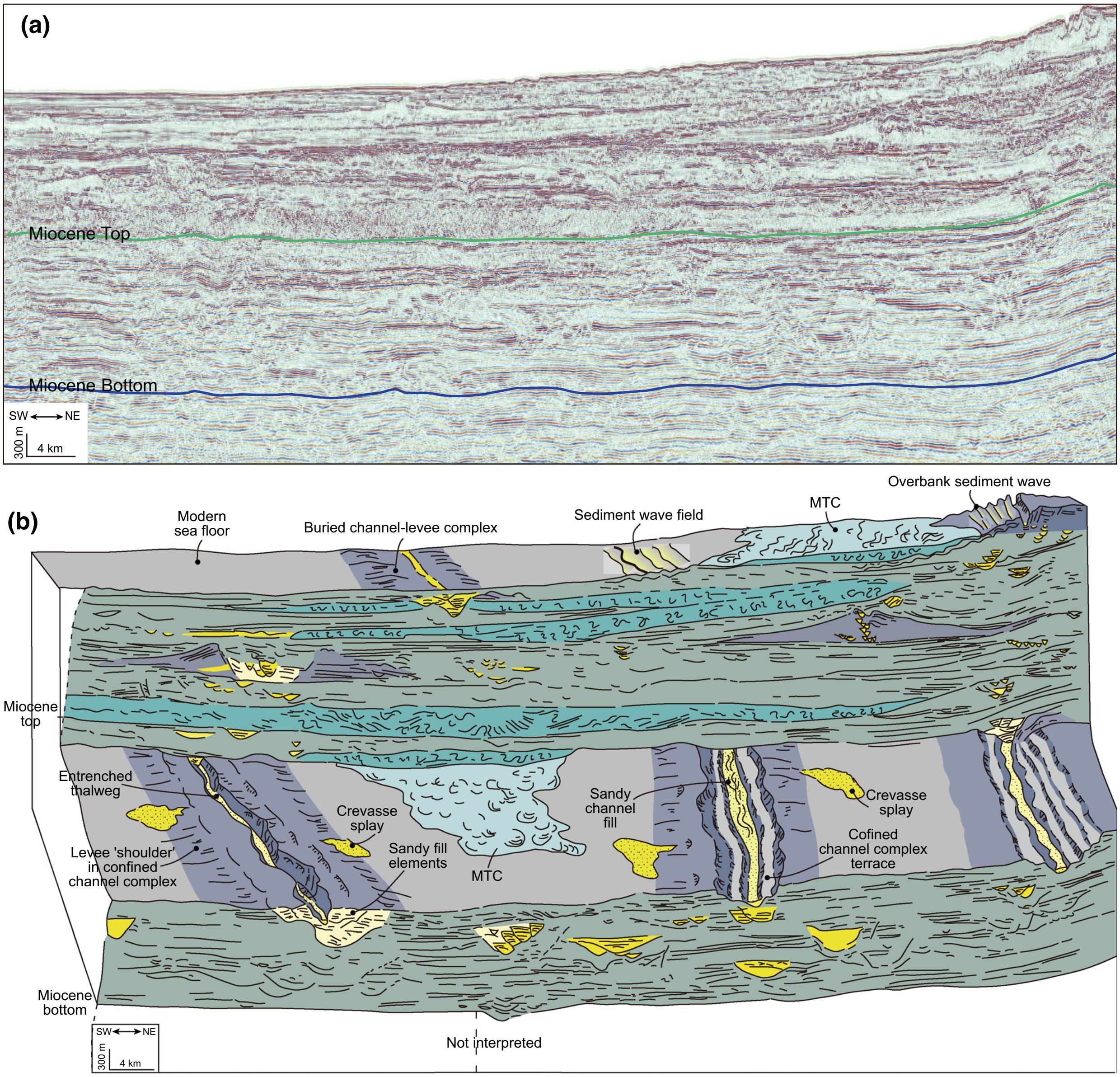

Fig. 14 A seismic transect (**a**) across the deep-water area in the Rakhine Basin and block schematic interpretation diagram (**b**) showing the architectural element evolution from the Miocene to the Pleistocene

may include that the Pliocene–Pleistocene deltaic sandstones (perhaps coming from both the north and the east) comprise the reservoirs, interbedded shales provide top seals and traps are associated with anticlines.

7 Conclusions

Six different types of architectural elements which vary in seismic characteristics, geometries, scales and fillings are recognized from the shelf to the slope and basin floor. The study area in the Oligocene–Middle/Late Miocene experienced rapid progradation of deep-water architectural elements, showing that the deposition varied from Eocene–Oligocene hemipelagic mudstone drape to Middle/Upper Miocene confined slope channel complex systems. The study area experienced gradual retrogradation and gradual progradation in the Middle/Late Miocene–Early Pliocene and Early Pliocene–Pleistocene, respectively, according to the vertical variation of the architectural elements observed in the seismic. Most of the sediments have been sourced from the Ganges–Brahmaputra fluvio-deltaic system to the north with only minor lateral input from the Indo-Burmese Ranges to the east.

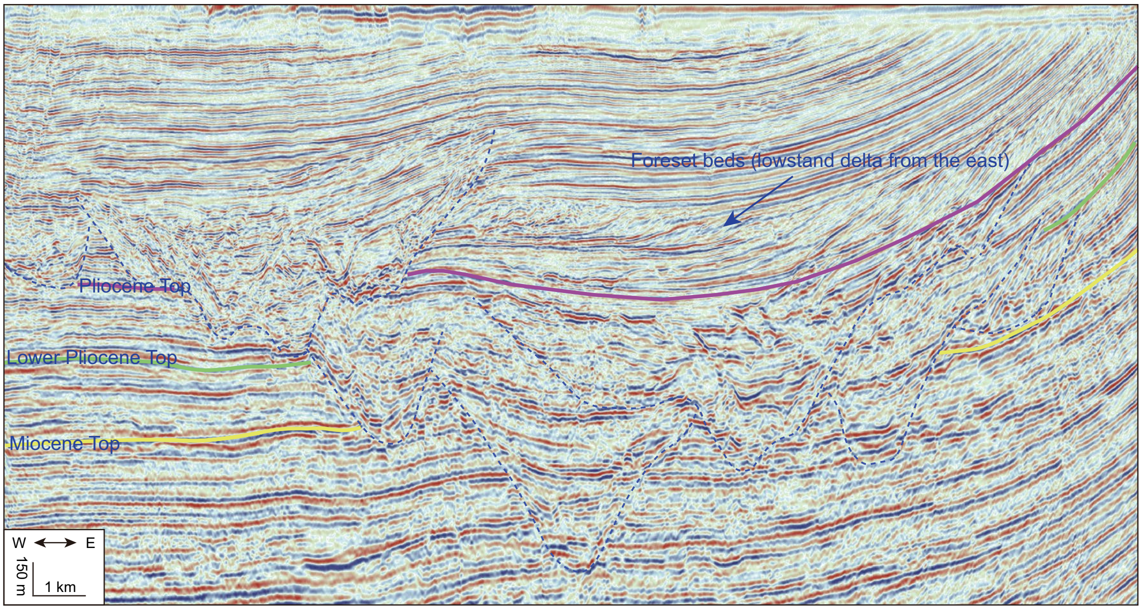

Fig. 15 A seismic transect through the shelf the area in the shelf Block AD6, showing the shelf canyons trending from north to south and the Pleistocene low-stand delta supplied from inland Myanmar

No matter relatively thick sands in frontal splays or thin sandstones in the levee-overbank, these sandstones were drilled to be gas bearing and have good reservoir quality. Drilling success indicates that the structural trap and trap effectiveness are very important in gas accumulation.

References

Belderson RH, Stride AH. The shape of submarine canyon heads revealed by Asdic. Deep-Sea Res. 1969;16(1):103–4. https://doi.org/10.1016/0011-7471(69)90055-2.

Belderson RH, Kenyon NH. Long-range sonar views of submarine canyons. Mar Geol. 1976;22(3):69–74. https://doi.org/10.1016/0025-3227(76)90043-8.

Cronin BT, Akmetzhanov AM, Mazzini A, Akhmanov G, Ivanov M, Kenyon NH. Morphology, evolution and fill: implications for sand and mud distribution in filling deep-water canyons and slope channel complexes. Sed Geol. 2005;179(1):71–97. https://doi.org/10.1016/j.sedgeo.2005.04.013.

Curray JR, Emmel FJ, Moore DG. The Bengal Fan: morphology, geometry, stratigraphy, history and processes. Mar Pet Geol. 2002;19(10):1191–223. https://doi.org/10.1016/S0264-8172(03)00035-7.

Damuth JE, Flood RD, Kowsmann RO, Belderson RH, Gorini MA. Anatomy and growth pattern of Amazon deep-sea fans as revealed by long-range side-scan sonar (GLORIA) and high-resolution seismic studies. AAPG Bull. 1988;72(8):885–911. https://doi.org/10.1029/JB093iB08p09211.

Gong CL, Wang YM, Steel RJ, Peakall J, Zhao X, Sun Q. Flow processes and sedimentation in unidirectionally migrating deep-water channels: from a three-dimensional seismic perspective. Sedimentology. 2016;63(3):645–61. https://doi.org/10.1111/sed.12233.

Gong CL, Wang YM, Rebesco M, Salon S, Steel RJ. How do turbidity flows interact with contour currents in unidirectionally migrating deep-water channels? Geology. 2018;46(6):551–4. https://doi.org/10.1130/G40204.1.

Hübscher C, Spieß V, Breitzke M, Weber ME. The youngest channel–levee system of the Bengal Fan: results from digital echosounder data. Mar Geol. 1997;141(1–4):125–45. https://doi.org/10.1016/S0025-3227(97)00066-2.

Janoko M, Nemec W, Henriksen S, Warchoł M. The diversity of deep-water sinuous channel belts and slope valley-fill complexes. Mar Pet Geol. 2013;41(1):7–34. https://doi.org/10.1016/j.marpetgeo.2012.06.012.

Jegou I, Savoye B, Pirmez C, Droz L. Channel-mouth lobe complex of the recent Amazon Fan: the missing piece. Mar Geol. 2008;252(1–2):62–77. https://doi.org/10.1016/j.margeo.2008.03.004.

Kang HQ, Meng JL, Cheng T, Huaicun JI, Bo BA, Minggang LI. Characteristics of deep water depositional system in Campos basin, Brazil. Pet Explor Dev. 2018;45(1):93–104. https://doi.org/10.11698/PED.2018.01.09 **(in Chinese)**.

Kneller B. The influence of flow parameters on turbidite slope channel architecture. Mar Pet Geol. 2003;20(6):901–10. https://doi.org/10.1016/j.marpetgeo.2003.03.001.

Kolla V, Coumes F. Morphology, internal Structure, seismic Stratigraphy, and sedimentation of Indus Fan. Deep Sea Research Part B

Oceangr Lit Rev. 1987;34(12):1045. https://doi.org/10.1016/.198-0254(87)95931-0.
Kolla V. A review of sinuous channel avulsion patterns in some major deep-sea fans and factors controlling them. Mar Pet Geol. 2007;24(6):450–69. https://doi.org/10.1016/j.marpetgeo.2007.01.004.
Lee SE, Talling PJ, Ernst GG, Hogg AJ. Occurrence an origin of submarine plunge pools at the base of the US continental slope. Mar Geol. 2002;185(3–4):365–77. https://doi.org/10.1016/S0025-3227(01)00298-5.
Li JR, Liu SF, Feng XL, Sun X, Shi X. Major and trace element geochemistry of the mid-Bay of Bengal surface sediments: implications for provenance. Acta Oceanol Sin. 2017a;36(3):82–90. https://doi.org/10.1007/s13131-017-1041-z1.
Li Q, Wu W, Yu S, Kang H, Tong L, Cao X, et al. The application of three-dimensional seismic spectral decomposition and semblance attribute to characterizing the deepwater channel depositional elements in the Taranaki Basin of New Zealand. Acta Oceanol Sin. 2017b;36(9):79–86. https://doi.org/10.1007/s13131-017-113-0.
Liu L, Zhang TS, Zhao XM, Wu S, Hu J, Wang X, et al. Sedimentary architecture models of deepwater turbidite channel systems in the Niger Delta continental slope, West Africa. Pet Sci. 2013;10(2):139–48. https://doi.org/10.1007/s12182-013-0261-x.
Ma HX, Lu FL, Fan GZ, Sun H, Gao CX. Seismic response and geological characteristics of mass-transport deposits in the Rakhine Basin, offshore Myanmar. Oil Gas Geol. 2011;32(54):751–9. https://doi.org/10.11743/ogg20110514 (**in Chinese**).
Pickering KT, Coleman J, Cremer M, Droz L, Kohl B, Normark W, et al. A high sinuosity, laterally migrating submarine fan channel–levee–overbank: results from DSDP Leg 96 on the Mississippi Fan, Gulf of Mexico. Mar Pet Geol. 1986;3(1):3–18. https://doi.org/10.1016/0264-8172(86)90052-8.
Twichell DC, Schwab WC, Kenyon NH. Geometry of sandy deposits at the distal edge of the Mississippi Fan, Gulf of Mexico. In: Pickering KT, Hiscott RN, Kenyon NH, RicciLucchi F, Smith RDA, editors. Atlas of deep water environments. Dordrecht: Springer; 1995. p. 282–6.
Pirmez C, Hiscott RN, Kronen JD. Sandy turbidite successions at the base of channel–levee systems of the Amazon Fan revealed by FMS logs and cores: unraveling the facies architecture of large submarine fans. Proc ODP Sci Results. 1997;155:7–33. https://doi.org/10.2973/odp.proc.sr.155.201.1997.
Qin ZL, Wu SG, Wang DW, Li W, Gong S, Mi L, et al. Mass transport deposits and processes in the north slope of the Xisha Trough, northern South China Sea. Acta Oceanol Sin. 2013;34(9):117–25. https://doi.org/10.1007/s13131-015-0608-9.
Racey A, Ridd MF. Petroleum geology of Myanmar. Geological Society Memoir No. 45. London: The Geological society; 2015. p. 93–108.
Saller A, Werner K, Sugiaman F, Cebastiant A, May R, Glenn D, et al. Characteristics of Pleistocene deep-water fan lobes and their application to an upper Miocene reservoir model, offshore East Kalimantan, Indonesia. AAPG Bull. 2008;92(7):919–49. https://doi.org/10.1306/03310807110.
Schwenk T, Spieβ V, Breitzke C, Hübscher C. The architecture and evolution of the Middle Bengal fan in vicinity of the active channel–levee system imaged by high-resolution seismic data. Mar Pet Geol. 2005;22(5):637–56. https://doi.org/10.1016/j.marpetgeo.2005.01.007.
Shanmugham G, Moiola RJ. Types of submarine fan lobes: models and implications. AAPG Bull. 1991;75(1):156–79. https://doi.org/10.1306/0C9B276D-1710-11D7-8645000102C1865D.
Sprague ARG, Garfield TR, Goulding FJ, Beaubouef RT, Sullivan MD, Rossen C, et al. Integrated slope channel depositional models: the key to successful prediction of reservoir presence and quality in Offshore West Africa. In: CIPM conference; 2005.
Subrahmanyam V, Krishna KS, Ramana MV. Murthy KS 2008, Marine geophysical investigations across the submarine canyon (Swatch-of-No-Ground), northern Bay of Bengal. Curr Sci. 2008;94(4):507–13. https://doi.org/10.1073/pnas.0800733105.
Twichell DC, Schwab WC, Nelson CH, Kenyon NH, Lee HJ. Characteristics of a sandy depositional lobe on the outer Mississippi Fan from SeaMARC 1A sidescan sonar images. Geology. 1992;20(8):689–92. https://doi.org/10.1130/0091-7613(1992)020%3c0689:COASDL%3e2.3.CO;2.
Weber ME, Wiedicke MH, Kudrass HR, Hübscher C, Erlenkeuser H. Active growth of the Bengal Fan during sea-level rise and highstand. Geology. 1997;25(4):315–8. https://doi.org/10.1130/0091-7613(1997)025%3c0315:AGOTBF%3e2.3.CO;2.
Weber ME, Wiedicke-Hombach M, Kudrass HR, Erlenkeuser H. Bengal Fan sediment transport activity and response to climate forcing inferred from sediment physical properties. Sed Geol. 2003;155(3–4):361–81. https://doi.org/10.1016/S0037-0738(02)00187-2.
Wu SG, Qin ZL, Wang DW, Peng XC, Wang ZJ, Yao GS. Seismic characteristics and triggering mechanism analysis of mass transport deposits in the northern continental slope of the South China Sea. Chin J Geophys. 2011;54(12):3184–95. https://doi.org/10.3969/j.issn.0001-5733.2011.12.018 (**in Chinese**).
Yang SU, Kim JW. Pliocene basin-floor fan sedimentation in the Bay of Bengal (offshore northwest Myanmar). Mar Pet Geol. 2014;49:45–59. https://doi.org/10.1016/j.marpetgeo.2013.09.007.
Xu S, Wang YM, Peng XC, Zou H, Qiu Y, Gong C, et al. Origin of Taiwan Canyon and its effects on deepwater sediment. Sci China Earth Sci. 2014;57(11):2769–80. https://doi.org/10.1007/s11430-014-4942-0.
Zhang LF, Pan M, Wang HL. Deepwater turbidite lobe deposits: a review of the research frontiers. Acta Geol Sinica (Engl Ed). 2017a;91(1):283–300. https://doi.org/10.1111/1755-6724.13078.
Zhang P, Mei LF, Xiong P, Hu X, Li R, Qiu H. Structural features and proto-type basin reconstruction of the Bay of Bengal Basin: a remnant ocean basin model. J Earth Sci. 2017b;28(4):666–82. https://doi.org/10.1007/s12583-017-0750-8.
Zhang WB, Duan TZ, Liu ZQ, Liu YF, Zhao L, Xu R. Architecture mode, sedimentary evolution and controlling factors of deepwater turbidity channels: a case study of the M Oilfield. Pet Sci. 2017c;14(3):493–506. https://doi.org/10.1007/s12182-017-0181-2.